Chelating Ether–Phosphine Complexes of the Cobalt Group Metals. Crystal Structures of Bis[benzylbis(2-ethoxyethyl)-phosphine]-bis(trifluoromethanesulfonato)cobalt(II) and -trichlororhodium(III)†

Steven J. Chadwell, Simon J. Coles, Peter G. Edwards* and Michael B. Hursthouse
Department of Chemistry, University of Wales, Cardiff, PO Box 912, Cardiff CF1 3TB, UK

New Group 9 metal complexes have been prepared using the trifunctional ligand benzylbis(2-ethoxyethyl)phosphine (L). Reactions of this potentially hemilabile ligand with $CoCl_2$, and $CoCl_2·6H_2O$ with $AgCF_3SO_3$, have been studied, resulting in the isolation of $[CoCl_2L_2]$ **1** and $[CoL_2(O_3SCF_3)_2]$ **2** respectively. In the former complex L acts as a monodentate P-bonding ligand with the metal adopting a tetrahedral geometry, but in the latter it acts as an O,P chelate. The crystal structure for **2** has been determined and shows the metal to have a distorted-octahedral geometry with *trans* ligands (P and O) and *trans* triflates. The $^{31}P-\{^1H\}$ NMR spectrum of **2** suggests the formation of a dimeric species in solution. Reactions of L with $RhCl_3·3H_2O$, $[\{RhCl(CO)_2\}_2]$ and $[\{RhCl(cod)\}_2]$ (cod = cycloocta-1,5-diene) resulted in the isolation of $[RhCl_3L_2]$ **3**, $[RhCl(CO)L_2]$ **4** and $[RhCl(cod)L]$ **5** respectively, where L acts as a monodentate P-bonding ligand in **4** and **5**. Complex **4** is shown to be *trans* by NMR studies. In **3** the ligand bonds as a monodentate phosphorus donor in one case and as a bidentate O,P chelate in the other. The crystal structure of **3** has been determined and shows the metal to have a slightly distorted-octahedral *mer* arrangement with *cis* phosphorus donors. The fluxional nature of this complex has been monitored by variable-temperature $^{31}P-\{^1H\}$ and ^1H NMR spectroscopy which shows that these ligands readily interchange at high temperatures. The iridium analogue of **5** has been prepared from $[\{IrCl(cod)\}_2]$ resulting in the isolation of $[IrCl(cod)L]$ **6**. The reaction of **3** with cyclohexene gave an unstable alkene complex **7** which could not be isolated, but was identified by variable-temperature $^{31}P-\{^1H\}$ NMR studies.

In recent years there has been considerable interest in the use of so-called hemilabile ligands, where the differing reactivities of the two types of donor present lead to applications in homogeneous catalysis, since the more labile donor can readily facilitate the creation of a vacant site for co-ordination by another substrate. Studies with a variety of phosphines having different donors have been undertaken, but the application of phosphorus–oxygen compounds, and especially phosphine–ethers,[1] is becoming increasingly important. Oxygen–phosphorus compounds have been shown to enhance selectivities in a variety of reactions such as the nickel-catalysed oligomerization and polymerization of ethene,[2] and in the carbonylation and hydrocarbonylation of methanol to oxygen-containing C_2 products such as ethanoic acid,[3,4] ethanal[4,5] or ethanol.[6] Preparations and applications of these types of compounds have been extensively reviewed.[1a]

We are interested in applications of complexes with hemilabile ligands in the catalysis of reactions of alkenes, and have recently reported the preparation of the potentially terdentate ligand benzylbis(2-ethoxyethyl)phosphine (L), and its complexes of metals of the nickel triad.[7] Here we describe its reactivity with metals of the cobalt triad and reactions of selected complexes with cyclohexene.

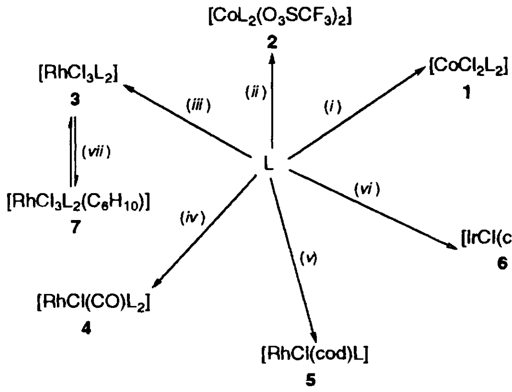

Scheme 1 (*i*) $CoCl_2$, CH_2Cl_2; (*ii*) $CoCl_2·6H_2O$, AgO_3SCF_3, EtOH; (*iii*) $RhCl_3·3H_2O$, EtOH; (*iv*) $[\{RhCl(CO)_2\}_2]$, C_6H_5Me; (*v*) $[\{RhCl(cod)\}_2]$, CH_2Cl_2; (*vi*) $[\{IrCl(cod)\}_2]$, C_6H_5Me; (*vii*) cyclohexene, $C_6D_5CD_3$

Results and Discussion

Cobalt Complexes.—Addition of the phosphine L to a suspension of $CoCl_2$ in dichloromethane results in the formation of $[CoCl_2L_2]$ **1** (Scheme 1) which can be isolated as a blue solid in good yield. The magnetic moment of 4.52 μ_B lies within the range expected for a tetrahedral cobalt(II) species (μ_{eff} = 4.4–4.8 μ_B)[8] and the analytical data (Table 1) are consistent with the proposed formulation. Tetrahedral cobalt(II) complexes with ether–phosphine ligands are known,[5] and are reported to be structurally similar to the analogous phosphine complexes $[CoX_2(PR_3)_2]$ (X = halide).[9] Attempts to reduce **1** by either sodium–mercury amalgam or potassium tris(but-2-yl)hydridoborate resulted in reactions from which no discrete products were obtained. It should be noted that the

---

† *Supplementary data available:* see Instructions for Authors, *J. Chem. Soc., Dalton Trans.*, 1995, Issue 1, pp. xxv–xxx.

Non-SI unit employed: $\mu_B \approx 9.27 \times 10^{-24}$ J T^{-1}.

bis(ligand) product **1** is preferentially formed even when insufficient ligand is used (1:1 stoichiometry, ligand:metal) indicating that chelation *via* the oxygen donor does not readily occur.

In order to encourage chelate formation on the cobalt(II) centre, abstraction of chloride from complex **1** was attempted by addition of an excess of either $AgBF_4$ or AgO_3SCF_3 resulting in the formation of pale pink solutions from which no discrete and readily identifiable complexes were isolated. However, the abstraction of chloride prior to the addition of L, by addition of silver triflate (AgO_3SCF_3) to a solution of cobalt(II) chloride, followed by addition of L to this mixture results in the formation of an air-sensitive pink crystalline solid **2**. Microanalysis indicated the composition to be $[CoL_2(O_3SCF_3)_2]$. The IR spectrum has been measured in solution (CCl_4) and as a Nujol mull, and shows the presence of both $CF_3SO_3^-$ and L. The infrared bands assigned to triflate are split, a feature that has previously been used to imply that triflate is co-ordinated.[10] The peak attributed to $\nu_{asym}(CF_3)$ is observed to shift to higher frequencies from free triflate in the solid-state spectrum (1260 to 1315 cm^{-1}) which also indicates co-ordination.[11] In the solution IR spectrum absorptions are observed at 1260 and 1313 cm^{-1} which implies the presence of free and co-ordinated triflate. Some other previous reports[12,13] propose to distinguish the mode of co-ordination of triflate (monodentate or bridging) by the complexity of the spectrum and a shift in the absorption, but the usefulness of this method has been questioned[11] and is certainly unreliable in the present case as assignments are difficult due to the inherent complexity caused by the L peaks. In the solid state the frequency assigned to $\nu_{asym}(C_2O)$ of the ether function in L can be seen at *ca.* 1100 cm^{-1}. In previous reports[1a,14] it has been stated that this frequency can be used to distinguish between mono- and bidentate ether-phosphines since $\nu_{asym}(C_2O)$ shifts to lower frequencies on formation of the M–O bond. In the solid-state IR spectrum for **2**, a noticeable shift is not observed or is masked by the broadness of the peak. However, in the higher-resolution solution spectrum (CCl_4) two absorptions assigned to $\nu_{asym}(C_2O)$ are observed (1122 and 1108 cm^{-1}) which indicates the presence of both co-ordinated and non-co-ordinated ether functions.

Table 1 Analytical and physical data

Complex	M.p./°C	Analysis (%)[a] C	Analysis (%)[a] H	μ_{eff}/μ_B
1 $[CoCl_2L_2]$	46–47	53.9 (54.1)	8.0 (7.6)	4.52
2 $[CoL_2(O_3SCF_3)_2]$[b]	124–127 (decomp.)	41.8 (43.0)	5.7 (5.6)	4.34[c]
3 $[RhCl_3L_2]$[d]	128–129	48.1 (48.3)	6.7 (6.8)	*e*
4 $[RhCl(CO)L_2]$	59–60	52.9 (53.0)	7.6 (7.2)	*e*
5 [RhCl(cod)L]	102–105	53.4 (53.7)	7.7 (7.2)	*e*
6 [IrCl(cod)L]	103–104	45.5 (45.7)	6.3 (6.2)	*e*

[a] Required values are given in parentheses. [b] Λ = 11.7 (CH_2Cl_2), 39.6 (EtOH) and 120.6 Ω^{-1} cm^2 mol^{-1} ($MeNO_2$). [c] Based on the monomeric unit. [d] Analysis performed by C.H.N. Analysis Ltd., Leicester; Cl, 14.2(14.3)%. [e] Diamagnetic.

Magnetic susceptibility shows that complex **2** is paramagnetic in the solid state, with a magnetic moment of 4.34 μ_B, which lies close to the range expected for high-spin octahedral cobalt(II) species (μ_{eff} = 4.8–5.2 μ_B at room temperature).[8] The $^{31}P-\{^1H\}$ NMR spectrum in chlorinated solvents ($CDCl_3$) shows a sharp singlet at room temperature (δ 13.25, $\nu_{\frac{1}{2}}$ = 40 Hz) (Table 2) which indicates that the product is diamagnetic in solution, and probably a dimer with a Co–Co bond. Diamagnetism in solution is confirmed by the bulk solution magnetic susceptibility at room temperature and by the Evans method.[15]

Variable-temperature $^{31}P-\{^1H\}$ NMR spectroscopy of complex **2** in $CDCl_3$ shows that the sharp singlet at *ca.* δ 13 is temperature invariant (−60 to +60 °C). However, in all isolated samples a residual minor impurity can be observed as two singlets (*ca.* δ −6 and −15) at low temperatures; the temperature at which the new peaks begin to appear is variable depending on the quality of the product (usually between −40 and −60 °C), and they are probably due to the presence of a cobalt(II) dimer. As the solution is warmed the peaks due to this minor impurity disappear which implies a monomer–dimer equilibrium for this species where the lifetime of the diamagnetic dimer becomes short at higher temperatures (relative to the NMR time-scale) and the influence of the paramagnetic monomer becomes dominant. The relative

Table 2 NMR spectroscopic data [δ, J(Hz)][a]

Complex	$^{31}P-\{^1H\}$	^1H	$^{13}C-\{^1H\}$
2[b]	13.25 (s)	Broad	114.9 (s, br, aryl), 129.2 (s, br, aryl), 142.4 (s, br, CF_3SO_3)[c]
3[d]	43.0 [dd, ^1J(Rh–P) = 127, ^2J(P–P) = 23], 39.3 [dd, ^1J(Rh–P) = 111, ^2J(P–P) = 23]	Broad	15.3 (s, CH_3), 22.7, 28.5, 29.9, 37.7, 39.0 (br, CH_2), 66.3 (br, OCH_2), 130.9 (br, aryl), 134.6 (br, aryl)
4[d]	16.5 [d, ^1J(Rh–P) = 121]	1.2 (t, CH_3), 2.2 (m, br, PCH_2CH_2), 3.4 (m, br, OCH_2CH_3), 3.7 (s, CH_2Ph), 3.9 (m, CH_2CH_2O), 7.1 (d, aryl), 7.2 (t, aryl), 7.6 (d, aryl)	15.4 (s, CH_3), 25.6 (s, br, PCH_2CH_2), 34.1 (s, br, CH_2Ph), 66.5 (s, CH_3CH_2O), 68.4 (s, CH_2CH_2O), 128–136 (aryl), 188.3 [d, br, ^1J(Rh–CO) = 73.25, CO]
5[e]	17.0 [d, ^1J(Rh–P) = 148]	1.1 (t, CH_3), 1.8–2.0 (m, CH_2, cod), 2.2 (m, PCH_2CH_2), 3.3 (m, OCH_2CH_3, =CH, cod), 3.5 (s, br, $PhCH_2$), 3.8–4.1 (m, br, CH_2CH_2O), 5.7 (s, br, =CH, cod), 7.1–7.8 (m, aryl)	16.5 (s, CH_3), 23.6 [d, ^1J(P–C) = 22, PCH_2CH_2], 31.5 [d, ^1J(P–C) = 19, PCH_2Ph], 29.9, 34.7 (s, CC=C, cod), 67.6 (s, CH_3CH_2O), 69.8 (CH_2CH_2O), 68.7, 68.8, 104.5 (C=C, cod), 128–137 (aryl)
6[e]	6.03 (s)	1.1 (t, CH_3), 1.6 (m, PCH_2CH_2), 1.8–2.2 (m, CH_2, cod), 3.2 (s, br, $PhCH_2$), 3.3–3.4 (m, OCH_2CH_3, =CH, cod), 3.7–4.0 (m, CH_2CH_2O), 5.3 (m, br, =CH, cod), 7.1 (t, aryl), 7.2 (t, aryl), 7.7 (d, aryl)	15.4 (s, CH_3), 22.4 [d, ^1J(P–C) = 31, PCH_2CH_2], 29.6 (s, br, CC=C, cod), 34.2 (s, CH_2Ph), 51.0 (s, CC=C, cod), 66.6 (s, CH_3CH_2O), 68.6 (s, CH_2CH_2O), 91.1, 91.8 (C=C, cod), 128–136 (aryl)[f]

[a] All at room temperature. Variable-temperature studies are detailed in the text and figures. [b] In $CDCl_3$. [c] All other peaks broadened into baseline. [d] In $C_6D_5CD_3$, except for $^{13}C-\{^1H\}$ (in C_6D_6). [e] In C_6D_6. [f] Gated ^{13}C NMR spectrum shows ^1J(C–H) = 153, 157 (C=C) and 143 Hz (CH_2O). All other couplings obscured.

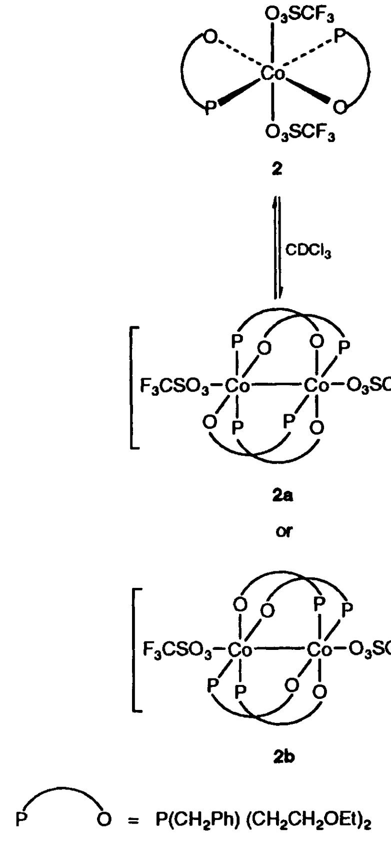

Scheme 2

concentration of this impurity is not enough for such a paramagnetic species to influence significantly the observed diamagnetic bulk susceptibility.

The variable-temperature ^{19}F NMR spectrum shows a broad singlet at δ −10.3 at room temperature ($\nu_{\frac{1}{2}}$ = 839 Hz) which sharpens at high temperatures ($\nu_{\frac{1}{2}}$ = 430 Hz). However, at low temperatures ($\leqslant -20$ °C) a second minor and broad resonance centred at *ca.* δ −50.0 ($\nu_{\frac{1}{2}}$ = *ca.* 1000 Hz) appears which is presumably associated with the impurity observed in the ^{31}P-{^{1}H} NMR spectrum. The ^{1}H NMR spectrum is broad and uninformative, as is the ^{13}C-{^{1}H} NMR spectrum, where resonances due to ligand aliphatic carbons are broadened into the baseline; the aryl carbons are observed (δ 115 and 129) as is a resonance attributed to triflate (δ 142).

Solution conductivity measurements implied partial dissociation of triflate in dichloromethane and ethanol. However, in nitromethane the conductivity suggests the presence of a three-ion species based on the dimeric unit, *i.e.* $[Co_2L_4(O_3SCF_3)_2]^{2+}$ 2 $O_3SCF_3^-$ with two free triflate anions (Λ = 241.2 Ω^{-1} cm^2 mol^{-1}). Thus, the NMR data together with the solution conductivity and IR studies indicate that complex **2** forms a dimer (dication) in solution, with magnetically equivalent phosphorus ligands. This enables us to propose likely structures for the cation (Scheme 2).

The single-crystal structure of complex **2** has been determined (Fig. 1, Tables 3 and 4). It confirms the formulation suggested by microanalysis, magnetic susceptibility and solid-state IR data. The metal has a distorted-octahedral geometry with *trans* chelating ligands (P and O donors) and *trans* triflate groups. The Co–O bond lengths of 2.103(4) and 2.114(4) Å for triflate and ligand respectively are close to values for other cobalt(II) complexes,[16,17] though the triflate bond is slightly longer than previously reported. However, the Co–P bond lengths [2.520(2) Å] are significantly longer than experimental values for other cobalt(II) phosphine complexes (2.2–2.3 Å)[18] indicating a relative weakening. Compression of the O(2)–Co–P(1) bond angle [79.78(12)°] shows chelate ring strain within the molecule, and is close to expected values.[19]

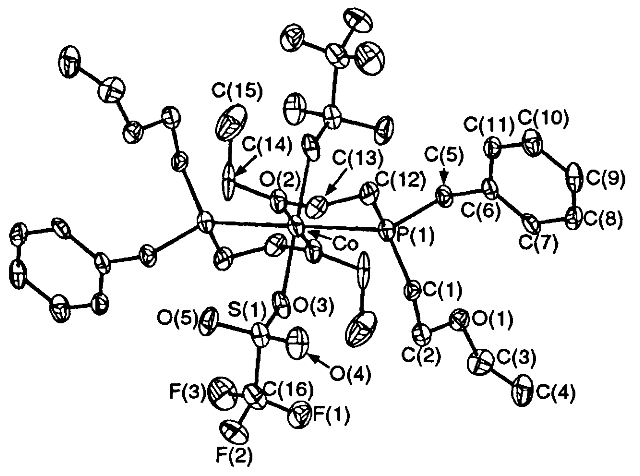

Fig. 1 Crystal structure of centrosymmetric $[CoL_2(O_3SCF_3)_2]$ **2**

Table 3 Selected bond lengths (Å) and angles (°) for $[CoL_2(O_3SCF_3)_2]$ **2**

Co–P(1)	2.520(2)	Co–O(3)	2.103(4)
Co–O(2)	2.114(4)		
O(3')–Co–P(1)	88.41(13)	O(3)–Co–O(3')	180.0
O(2)–Co–P(1)	79.78(12)	O(2)–Co–O(2')	180.0
O(3)–Co–O(2)	92.6(2)	C(12)–P(1)–Co	95.0(2)
O(3)–Co–O(2')	87.4(2)	C(13)–O(2)–Co	121.2(3)
O(3)–Co–P(1)	91.59(13)	P(1)–Co–P(1')	180.0
O(2')–Co–P(1)	100.22(12)	C(1)–P(1)–Co	121.6(2)
		C(14)–O(2)–Co	127.3(4)

There are significant differences between the angles around the co-ordinated donors. The Co–P(1)–C(12) angle of 95.0(2)° is considerably smaller than would be expected for an unrestricted tertiary phosphine phosphorus centre,[20] and is significantly compressed compared with the corresponding angle in the non-chelating ether arm [Co–P(1)–C(1) 121.6(2)°]. The oxygen of the chelate donor does not exhibit a similar distortion, where the corresponding angle [Co–O(2)–C(13) 121.2(3)°] is similar to the non-chelating ether angle [Co–O(2)–C(14) 127.3(4)°]. This distortion results in an effective rotation of the tertiary phosphine function about the axis required for maximal Co–P bonding and towards the chelating oxygen. As a result it appears that the Co–P(1)–C(12) angle is compressed in order to accommodate the ether in a more ideal bonding position and at the expense of Co–P bonding. These data suggest that the structural distortions are more dependent upon constraints imposed by the chelating ligands rather than electronic factors such as a Jahn–Teller distortion in this d^7 complex. Complex **2** does not appear to react with cyclohexene since the ^{31}P-{^{1}H} NMR spectrum does not change for an *in situ* reaction mixture (−60 to +60 °C).

Rhodium Complexes.—The reaction of 1, 2 or 3 mole equivalents of the phosphine L with rhodium trichloride results in orange crystalline $[RhCl_3L_2]$ **3** in high yield. Complex **3** was characterized by microanalysis, and ^{31}P-{^{1}H} NMR data (162 MHz, 263 K), which clearly show two phosphorus environments in an ABX pattern (X = ^{103}Rh). In addition to rhodium–phosphorus coupling [^1J(Rh–P) = 111, ^1J(Rh–P') = 127 Hz], phosphorus–phosphorus coupling is also observed [^2J(P–P) =

Table 4 Atomic coordinates (× 10^4) for $[CoL_2(O_3SCF_3)_2]$ **2**

Atom	x	y	z
Co	5000	0	5000
F(1)	2578(4)	−1200(3)	2250(3)
F(2)	2807(4)	216(4)	1337(2)
F(3)	4181(4)	−883(4)	1931(3)
S(1)	3587(2)	737(2)	2985(1)
P(1)	3231(1)	44(2)	5651(1)
O(1)	1605(4)	−2190(4)	5050(3)
O(2)	4758(4)	1905(3)	5077(3)
O(3)	4089(3)	−94(4)	3689(3)
O(4)	2524(4)	1220(4)	3110(3)
O(5)	4330(4)	1580(4)	2704(3)
C(1)	1844(5)	−41(6)	4936(4)
C(2)	1582(6)	−1213(5)	4438(4)
C(3)	1086(6)	−3257(5)	4667(5)
C(4)	−173(6)	−3191(6)	4556(5)
C(5)	3068(5)	−699(5)	6691(4)
C(6)	2120(6)	−268(5)	7127(4)
C(7)	1121(6)	−895(6)	6973(4)
C(8)	225(6)	−490(6)	7364(4)
C(9)	314(6)	547(6)	7890(5)
C(10)	1326(7)	1154(6)	8030(5)
C(11)	2202(6)	739(6)	7682(4)
C(12)	3326(6)	1654(5)	5933(4)
C(13)	3704(5)	2406(5)	5237(5)
C(14)	5509(6)	2861(6)	4897(5)
C(15)	6034(7)	3529(6)	5748(6)
C(16)	3263(7)	−346(6)	2094(5)

23 Hz] and is typical for a *cis* P–M–P interaction.[21] The room-temperature ^1H NMR spectrum is broad as is the $^{13}C-\{^1H\}$ NMR spectrum, and neither resolve chelating and non-chelating ether functions. The IR spectrum shows an intense absorption at 1103 cm^{-1}, which can be attributed to $\nu_{asym}(C_2O)$. This does not distinguish between the chelating and non-chelating ligands as has previously been observed for similar compounds;[14] the solution IR spectrum (CCl_4), however, shows two peaks assigned to $\nu_{asym}(C_2O)$ at 1126 and 1104 cm^{-1}, indicating both chelating and non-chelating ether groups.

The variable-temperature $^{31}P-\{^1H\}$ and ^1H NMR spectra of complex **3** indicate fluxionality. In the low-temperature $^{31}P-\{^1H\}$ NMR spectrum (Fig. 2). a pattern consisting of two overlapping doublets of doublets arises, indicating an ABX spin system (X = ^{103}Rh). Upon warming, this pattern begins to collapse (−20 °C), and around room temperature the signal broadens; coalescence is observed at *ca.* +40 °C where the signal appears as a broad triplet. As the solution is warmed further a doublet is observed at δ 37.85 [^1J(Rh–P) = 119 Hz]. This behaviour indicates a fluxional process whereby the phosphorus atoms exchange. Line-shape analysis allows estimation of ΔG for this process (62.5 ± 0.5 KJ mol^{-1}) which may be compared with values found for the analogous phosphine–ester $Ph_2PCH_2C(O)OEt$ (64.3 ± 0.5 kJ mol^{-1})[22] and ketophosphine $Ph_2PCH_2C(O)Ph$ (75 ± 2 kJ mol^{-1})[23] complexes. These activation parameters have been used to infer metal–oxygen bond strengths; in which case by comparison with these previous examples the oxygen–rhodium bond is weaker for the chelating ether in **3** than it is for chelating ketone and ester oxygens, as may be expected.

Variable-temperature ^1H NMR data have also been obtained for complex **3**. Again the spectrum changes over the entire temperature range of −100 to +100 °C in $[^2H_8]$ toluene. The changes observed at low temperatures are minor, and are consistent with some settling between alternative conformations of the ether arms ($\lambda \longleftrightarrow \delta$) and of the phenyl groups on the ligand and for which differences in energy are small. As the temperature is increased the peaks due to the CH_2 and CH_3 groups change. At low temperatures ($\leqslant$283 K) three triplets are observed in the methyl region in the ratio 1:2:1 from high to

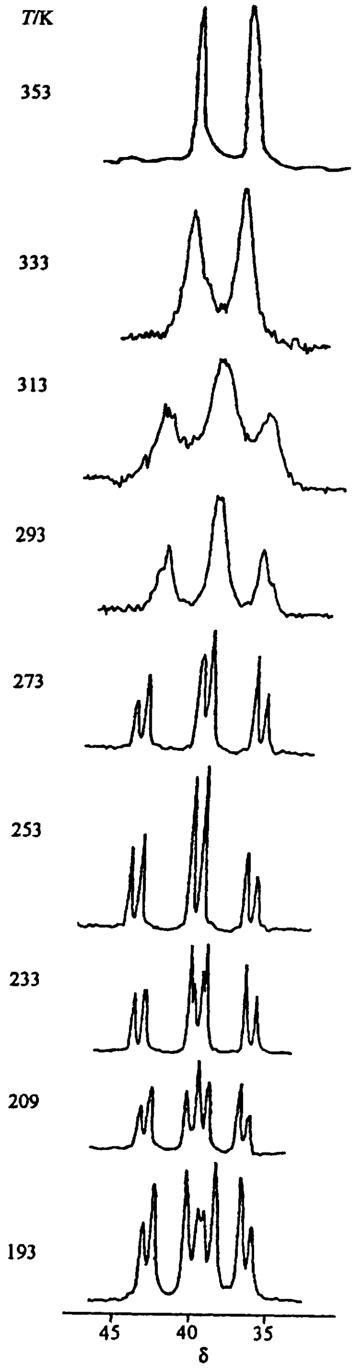

Fig. 2 Variable-temperature $^{31}P-\{^1H\}$ NMR spectra for $[RhCl_3L_2]$ **3**

low field, which correspond to ligand A (non-chelate) : ligand B : ligand A (chelate) where ligand A is O, P chelating and ligand B is phosphorus bonded. As the temperature is increased these triplets broaden and at room temperature (295 K) the methyl resonances attributed to the non-chelating ether arm in ligand A and the non-chelating ligand (B) coalesce. As the solution is warmed further (313 K) the resonance attributed to the chelating ether function in ligand A coalesces with this resonance to give one broad resonance which on further warming (> 363 K) sharpens to a triplet. In the CH_2 region, at low temperatures, many resonances with complex coupling can be seen, which on warming broaden and coalesce to give four broad peaks. These can be attributed to the four types of CH_2 environments in the ligand in the rapidly fluxional state, PCH_2CH_2 (δ 2.3), $PhCH_2$ (δ 3.5), OCH_2CH_3 (δ 3.7) and

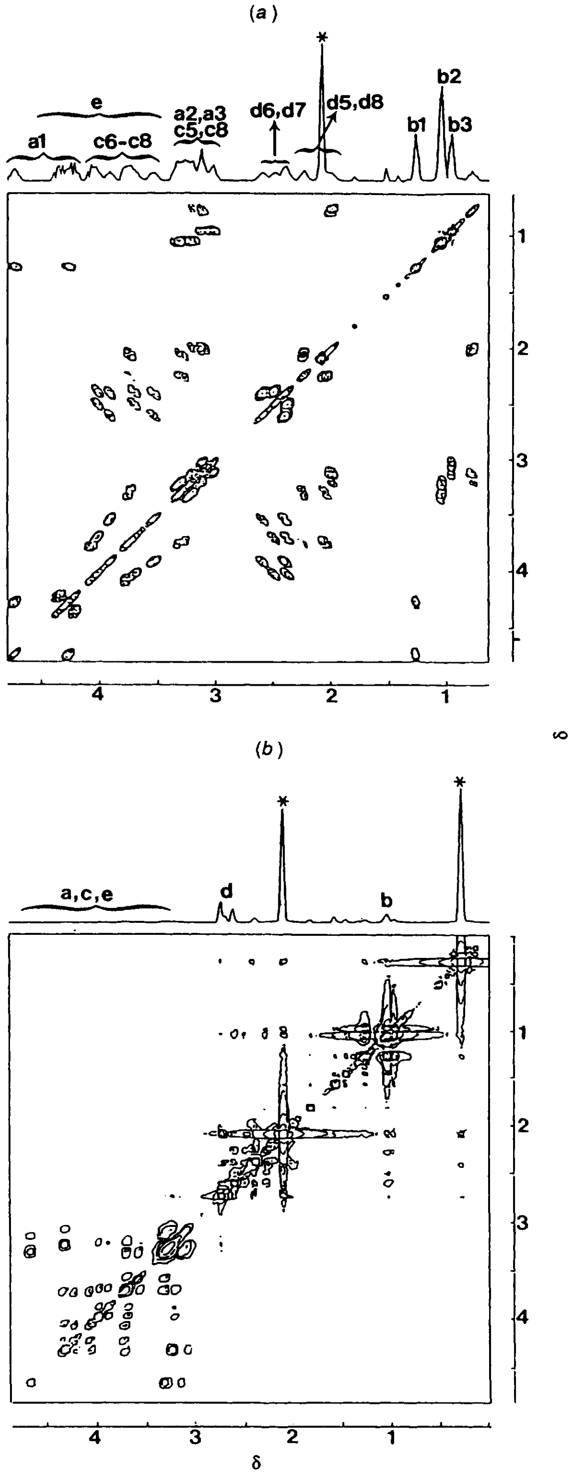

Fig. 3 Two-dimensional COSY (*a*) and EXSY (*b*) ^{1}H NMR spectra for [$RhCl_3L_2$] **3** (taken at 263 and 296 K respectively). N.B. Assignment of spins in the ligand fragment: $PhCH^e_2PCH^d_2CH^c_2OCH^a_2CH^b_3$. The asterisked peaks are due to solvent and impurity

OCH_2CH_2 (δ 4.0). This behaviour again indicates free exchange between ligands and is consistent with the $^{31}P\{^1H\}$ NMR spectra.

Since the changes which occur below room temperature are difficult to follow in the one-dimensional spectra, two-dimensional correlation (COSY) and exchange (EXSY) ^{1}H spectroscopy were used to assign the spectrum and exchanging spins. The COSY spectrum at 263 K [Fig. 3(*a*)] allows peak assignments to be made, and clearly shows that spins of type a are coupled with the respective spins of type b (*e.g.*, a1 couples with b1, *etc.*). Similarly, spins of type c are observed to couple with spins of type d (*e.g.*, c5 couples with d5, *etc.*). The spectrum cannot be used to distinguish which benzyl or ethyl fragments (protons of type c–e) are coupled with which dimethylene groups (a and b). It should also be noted that the methylene protons are magnetically inequivalent (*i.e.*, a1 and a1′, c5 and c5′, *etc.*), and the spectrum shows that these spins are also coupled with each other as expected. The CH_2CH_3 protons can be assigned at δ 4.3 and 4.7 (chelate, ligand A), 3.2 (ligand B) and 3.0 (non-chelate, ligand A); two discrete resonances are observed for the CH_2CH_3 protons in the chelating ether arm, indicating that they are magnetically inequivalent at this temperature. This is not observed for the non-chelating ether functions, presumably due to relatively free C–C bond rotation.

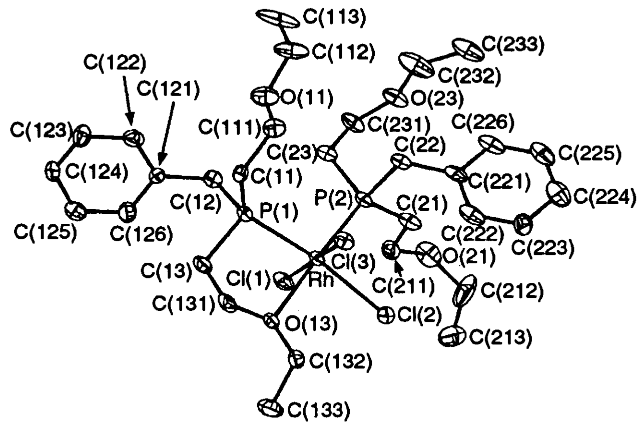

Fig. 4 Crystal structure of [$RhCl_3L_2$] **3**

Table 5 Selected bond lengths (Å) and angles (°) for [$RhCl_3L_2$] **3**

Rh–P(1)	2.294(2)	Rh–P(2)	2.249(2)
Rh–O(13)	2.281(4)	Rh–Cl(1)	2.332(2)
Rh–Cl(2)	2.399(2)	Rh–Cl(3)	2.349(2)
P(2)–Rh–O(13)	176.78(12)	P(2)–Rh–P(1)	100.25(6)
O(13)–Rh–P(1)	82.24(11)	P(2)–Rh–Cl(1)	89.31(7)
O(13)–Rh–Cl(1)	88.78(12)	P(1)–Rh–Cl(1)	86.89(6)
P(2)–Rh–Cl(3)	96.89(6)	O(13)–Rh–Cl(3)	85.09(12)
P(1)–Rh–Cl(3)	90.64(6)	Cl(1)–Rh–Cl(3)	173.65(6)
P(2)–Rh–Cl(2)	87.77(6)	O(13)–Rh–Cl(2)	89.70(11)
P(1)–Rh–Cl(2)	171.89(6)	Cl(1)–Rh–Cl(2)	92.06(6)
Cl(3)–Rh–Cl(2)	89.57(6)	C(11)–P(1)–Rh	118.9(2)
C(13)–P(1)–Rh	99.8(2)	C(132)–O(13)–Rh	119.5(3)
C(131)–O(13)–Rh	113.1(3)		

Two-dimensional COSY NMR spectroscopy cannot distinguish feasible exchange mechanisms for this fluxional process, however the room-temperature EXSY spectrum [Fig. 3(*b*)] clearly shows that all spins of a given type are in exchange with one another. This is most clearly seen in the methyl region, where b1 exchanges with b2 and b3, and b2 with b3 (*i.e.*, three cross-peaks). This can also be observed in the methylene region so that, for example, all spins of type a are seen to exchange with one another. Hence the exchange process is explained by co-ordinated for unco-ordinated ether exchange (arm on/arm off) during which the phosphorus atoms are also equilibrated.

The single-crystal structure of complex **3** has been determined (Fig. 4, Tables 5 and 6), and is consistent with the solution structure inferred from low-temperature NMR data. The rhodium(III) centre has a distorted *mer* octahedral arrangement. Bond lengths and angles are similar to literature values for similar complexes.[21c,24] Compression of the P(1)–Rh–O(13) angle [82.24(11)°] indicates chelate ring strain.

This is within expected values for this type of complex and for related phosphorus–nitrogen systems.[19,21c] A relative compression of the Rh–P(1)–C(13) bond angle in the chelate ring [99.8(2)°] compared with the non-chelate angles Rh–P(1)–C(11) [118.9(2)°], Rh–P(2)–C(22) [112.9(2)°] and Rh–P(2)–C(23) [113.4(2)°] can also be seen, but this effect is less pronounced than in complex **2**. This may be expected since rhodium(III) is more likely to prefer bonding to phosphorus in tertiary phosphines than is cobalt(II), so the predominance of the metal–oxygen bond is decreased. The terminal chloride ligands Cl(1), Cl(2) and Cl(3) have meridional geometry, which is precedented for rhodium(III) complexes with phosphorus–oxygen ligands,[23] and the ligand phosphorus atoms P(1) and P(2) are *cis* as is the case in solution (^{31}P NMR spectrum). The Rh–P bond *trans* to Cl[2.294(2) Å] is longer than the Rh–P bond *trans* to O [2.249(2) Å], consistent with a greater *trans* influence of chloride. The Rh–Cl bond *trans* to phosphorus [2.399(2) Å] is longer than that *trans* to chloride [2.332(2) Å] indicating a larger *trans* influence for phosphorus, presumably due to Rh–P π bonding. Thus the *trans* influences of the three donors fall in the series O < Cl < P.

Addition of cyclohexene to a solution of complex **3** in dichloromethane affords yellow solutions from which only **3** can be isolated, although formation of a labile adduct in solution is confirmed by variable-temperature ^{31}P-{^{1}H} NMR spectra (Fig. 5). At ambient temperature the NMR spectrum is identical to that observed for **3** (*cf.* Fig. 2), however, at lower temperatures ($\leqslant -20$ °C) the peaks slowly collapse and at -100 °C a doublet is resolved at *ca.* δ 45 [separation of peaks = 102 Hz, presumably ^1J(Rh–P)] indicating the formation of a new complex with co-ordinated alkene, *i.e.* [$RhCl_3L_2(C_6H_{10})$] **7**. This implies that the phosphorus atoms are equivalent; P–P coupling is not observed, however *cis* P–P coupling is small[21] and any potential *cis* P–P coupling would be obscured by the broadness of the peaks. The *trans* isomer would have equivalent phosphorus atoms for which coupling would not occur; in this case the broadness may be caused by a fluxional process that is not frozen at the low-temperature limit. Since complexes of the type $RhCl_3L_3$ are typically meridional, it is reasonable to suppose that **7** will also have a meridional arrangement of chloride ligands. Possible structures for **7** are shown in **a** and **b** where the alkene replaces the co-ordinated ether in **3**, and complexes **3** and **7** are in dynamic equilibrium. If meridional stereochemistry is maintained the phosphines will be inequivalent irrespective of the intermediate formed during a dissociative substitution of ether for alkene. It is also likely that the stereochemistry will be maintained if the mechanism of substitution requires associative activation, again resulting in inequivalent phosphines. Hence we favour structure **a**.

The rhodium(I) complex[$RhCl(CO)L_2$] **4** can be prepared by addition of L to a solution of [{Rh(μ-Cl)(CO)$_2$}$_2$]. The product was characterized by microanalysis, IR and NMR data, and the rhodium centre presumably has a square-planar geometry. The ^{31}P-{^{1}H} NMR spectrum shows a doublet centred at δ 16.5 [^1J(Rh–P) = 121 Hz], and no *cis* P–P coupling is seen, *i.e.* the two phosphorus environments are equivalent and must be *trans*. The NMR spectra are temperature invariant (-100 to $+100$ °C). The ^{1}H NMR spectrum can be assigned on the basis of intensities and chemical shifts, as can the ^{13}C-{^{1}H} NMR, where a broad weak resonance assigned to CO is observed at δ 188.3 [^1J(Rh–CO) = 73.25 Hz]. This coupling is within expected values for other rhodium(I) carbonyl complexes;[25] ^2J(P–C) coupling is not observed due to the broadness of the peaks. The IR spectrum shows the presence of CO (1967 cm^{-1}), L [$\nu_{asym}(C_2O)$ 1105 cm^{-1}] and Rh–Cl (305w cm^{-1}). Phosphine complexes of this type are well known[14,26] and it should be noted that **4** is formed on addition of 1, 2 or 3 mol of L relative to metal, showing that this is the preferred product even if a deficiency of phosphine ligand is used.

Attempts to cause dissociation of CO by UV irradiation or by heating both proved unsuccessful, and we have not observed

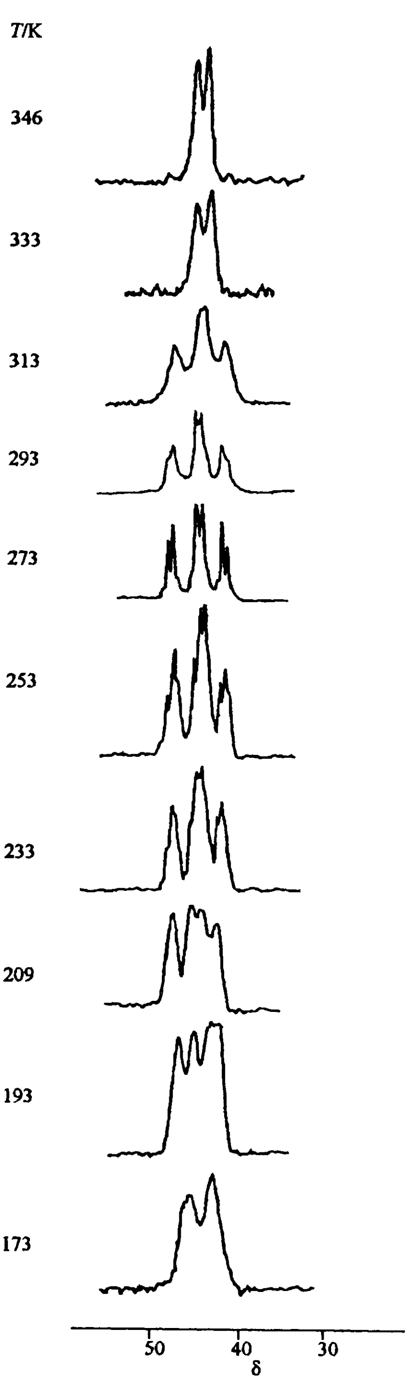

Fig. 5 Variable-temperature ^{31}P-{^{1}H} NMR spectra for [$RhCl_3L_2$] **3** + cyclohexene

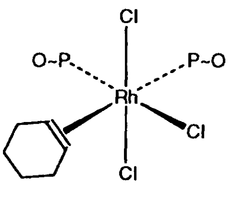

a

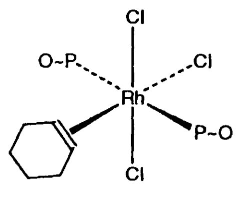

b

P~O = P-bonded $P(CH_2Ph)(CH_2CH_2OEt)_2$

O,P chelate formation. Chloride abstraction with silver tetrafluoroborate or silver triflate also did not result in the formation of pure isolable products in which O,P chelation could be observed, although reactions can be seen to occur by $^{31}P-\{^1H\}$ NMR spectroscopy.

The rhodium(I) complex [RhCl(cod)L] **5** (cod = cycloocta-1,5-diene) can be prepared by addition of 1 mol of L to a solution of $[\{Rh(\mu-Cl)(cod)\}_2]$. Microanalysis, mass spectrometry and IR suggests the formulation shown, and peaks in the NMR (^{31}P, ^1H and ^{13}C) can be assigned according to chemical shifts and intensities, and again the NMR spectra are temperature invariant. The ligand L bonds as a monodentate phosphorus donor. Presumably the ligand is *cis* to chloride in order to accommodate the chelating cod ligand. Again, attempts to form O,P chelates by chloride abstraction using silver salts did not result in the isolation of any discrete product, though a reaction can be seen to occur by $^{31}P-\{^1H\}$ NMR spectroscopy. Attempts to abstract cod by refluxing a solution of **5** with L gave a mixture of unidentified products ($^{31}P-\{^1H\}$ NMR spectroscopy) and reactions of L with other rhodium(I) starting materials such as $[\{RhCl(C_2H_4)_2\}_2]$, $[Rh(\eta-C_5H_5)(C_2H_4)_2]$ and $[\{RhCl(C_8H_{14})\}_2]$ also did not result in the isolation of any discrete complexes.

Iridium Complexes.—The iridium(I) analogue of complex **5** can be prepared in the same way to yield orange air-stable crystals of [IrCl(cod)L] **6**. As with **5**, microanalysis and IR suggests the formulation shown, and peaks in the NMR (^{31}P, ^1H and ^{13}C) can be assigned according to chemical shifts and intensities.

Attempts to abstract chloride from complex **6** using silver triflate and silver tetrafluoroborate resulted in a reaction (as observed by $^{31}P-\{^1H\}$ NMR spectroscopy), but it has not proved possible to isolate a pure product. An attempt to substitute cod by refluxing with an excess of L also appeared to result in a reaction (by $^{31}P-\{^1H\}$ NMR), but again no discrete complex was isolated. The phosphine does not react with Vaska's compound $[IrCl(CO)(PPh_3)_2]$ (toluene, reflux). Reactions with $IrCl_3 \cdot 3H_2O$ give rise to mixtures of products; the iridium analogue of **3** could not be isolated.

Experimental

All syntheses described were carried out under strictly anaerobic conditions using a Halco Engineering 140 FF glove-box, or standard vacuum-line techniques. All solvents were refluxed under N_2 over sodium–benzophenone and distilled immediately prior to use, except for ethanol and dichloromethane which were dried over CaH_2 and toluene which was dried over sodium. The metal chlorides and silver salts were used as received, except for $CoCl_2$ which was dried *in vacuo* (180 °C, 8 h). Benzylbis(2-ethoxyethyl)phosphine was prepared as previously described,[7] as were the starting materials, $[\{Rh(\mu-Cl)(CO)_2\}_2]$,[27] $[\{Rh(\mu-Cl)(cod)\}_2]$[28] and $[\{Ir(\mu-Cl)(cod)\}]_2$.[29]

Photolyses were performed with a Hanovia 50 W medium-pressure mercury lamp in quartz glassware. The NMR spectra were recorded on a Bruker WM-360 spectrometer operating at 360.134 (^1H) or 90.560 MHz (^{13}C), a JEOL FX-90Q operating at 89.55 (^1H), 36.23 (^{31}P), 22.49 (^{13}C) or 84.25 MHz (^{19}F), or by the EPSRC service at Warwick on a Bruker ACT 400 spectrometer operating at 161.978 (^{31}P) or 400.134 MHz (^1H). Spectra were referenced externally to 85% H_3PO_4 (^{31}P), $SiMe_4$ (^1H) or CF_3CO_2H [δ −76.55 relative to $CFCl_3$ (δ 0)] (^{19}F), or internally to solvent carbons (C_6D_6, δ 128.0; $CDCl_3$, δ 76.9) (^{13}C). The COSY-45 and EXSY-90 $^1H-^1H$ two-dimensional NMR spectroscopy was carried out on the Bruker ACT 400 instrument using the program COSY or EXSY from the standard Bruker software. For the COSY-45 spectrum, in the F2 dimension, 1024 data points were collected over 2959 Hz, and in F1 256 data points over 2959 Hz. Transformation was carried out with zero-filling to 512 points in F1, after application of a sine-bell multiplication applied to the time-domain data in both dimensions. The 45° acquisition pulse length was 5.5 μs and a delay of 0.8 s was applied between acquisitions. For the EXSY-90 spectrum, in the F2 dimension, 1024 data points were collected over 1953 Hz, and in F1 128 data points over 1953 Hz. Transformation was carried out as above. The 90° acquisition pulse length was 11 μs and a delay of 1.4 s was applied between acquisitions. Infrared data were obtained from a Nicolet 510 FT-IR in conjunction with a 620 processor or from a Perkin-Elmer 783 spectrophotometer, and referenced externally to polystyrene (1601 cm^{-1}). Unless otherwise stated, elemental analyses were performed in this department on a Perkin-Elmer 240C elemental analyser. Magnetic susceptibilities of solids (and for a solution of complex **2**) were obtained from a Sherwood Scientific magnetic susceptibility balance or by the Evans method in solution (see Discussion).[15] Conductivity data were obtained from a PTI-18 digital conductivity meter, and referenced against a standard solution of 1 mol dm^{-3} KCl. Mass spectrometry data were collected from a Fisons VG Platform II mass spectrometer or at the EPSRC service at University College, Swansea. Melting points were measured in sealed glass capillaries and are uncorrected.

Preparations.—*Bis[benzylbis(2-ethoxyethyl)phosphine]-dichlorocobalt*(II) **1**. To a suspension of $CoCl_2$ (0.42 g, 3.2 mmol) in dichloromethane (50 cm^3) was added a standard solution of phosphine L in light petroleum (b.p. 40–60 °C; 6.6 cm^3, 6.5 mmol) and the mixture allowed to stir (48 h), yielding a deep blue solution. The solvents were removed *in vacuo* and the residue extracted into hot light petroleum (200 cm^3). After concentration of this solution to saturation, complex **1** was isolated as a moderately air-sensitive pale blue solid in good yield (1.83 g, 85%). IR (Nujol mull): $\nu_{asym}(C_2O)$ 1103s; ν(M–Cl) 290w, 310w cm^{-1}.

Bis[benzylbis(2-ethoxyethyl)phosphine]bis(trifluoromethane-sulfonato)cobalt(II) **2**. To a solution of $CoCl_2 \cdot 6H_2O$ (0.52 g, 2.19 mmol) in ethanol (50 cm^3) was added AgO_3SCF_3 (1.12 g, 4.37 mmol) to give a pale pink solution with a white precipitate (AgCl). After filtering this solution, a standard solution of L (4.5 cm^3, 4.37 mmol) was added and the mixture allowed to stir (12 h) during which time it changed to orange. The solvents were removed *in vacuo* and the oil/solid residue was washed with light petroleum (4 × 10 cm^3) and extracted into dichloromethane (50 cm^3). After concentration of this solution to saturation, complex **2** was isolated as air-sensitive pink prisms in good yield. It was recrystallized from either dichloromethane or dichloromethane–light petroleum (*ca.* 5:1). $\delta_F(CDCl_3)$ −10.3 (s, br, $\nu_{\frac{1}{2}}$ = 839 Hz). IR: (Nujol mull) $\nu_{asym}(C_2O)$ 1100s; $\nu_{sym}(CF_3)$ 1215s, 1235s; $\nu_{asym}(CF_3)$ 1315s; $\nu_{sym}(SO_3)$ 1160s, 1165s, 1175s; $\nu_{asym}(SO_3)$ 1030s, 1045s, 1055s; ν(CS) 635vs; (CCl_4) $\nu_{asym}(C_2O)$ 1108s, 1122s; $\nu_{sym}(CF_3)$ 1215s, 1237s; $\nu_{asym}(CF_3)$ 1313s, 1260m; $\nu_{sym}(SO_3)$ 1171s(br); $\nu_{asym}(SO_3)$ 1029s, 1064w; ν(CS) 638vs cm^{-1}.

Bis[benzylbis(2-ethoxyethyl)phosphine]trichlororhodium(III) **3**. To a solution of $RhCl_3 \cdot 3H_2O$ (0.25 g, 0.95 mmol) in ethanol (40 cm^3) was added a standard solution of L in light petroleum (1.9 cm^3, 1.9 mmol), immediately yielding an orange solution. The solvents were removed *in vacuo* and the residue extracted into hot diethyl ether (250 cm^3). After concentration of this solution to saturation (*ca.* 50 cm^3) an air-stable pale orange precipitate of complex **3** was isolated in excellent yield (0.66 g, 93%). It was recrystallized as pale orange needles from diethyl ether. Mass spectrum [FAB, electron impact (EI), chemical ionization (CI)] (no M^+ observed): *m/z* 709/711 (*M* − Cl), 674 (*M* − 2Cl), 639 (*M* − 3Cl), 269 (L) and 91 ($PhCH_2$). IR:(Nujol mull) $\nu_{asym}(C_2O)$ 1103vs; (CCl_4) $\nu_{asym}(C_2O)$ 1126s, 1104s cm^{-1}.

Bis[benzylbis(2-ethoxyethyl)phosphine]carbonylchlororhodium(I) **4**. To a solution of $[\{RhCl(CO)_2\}_2]$ (0.21 g, 0.54 mmol)

Table 6 Atomic coordinates (× 10^4) for $[RhCl_3L_2]$ **3**

Atom	*x*	*y*	*z*	Atom	*x*	*y*	*z*
Rh	5 034(1)	3 385(1)	5 010(1)	C(122)	9 852(6)	3 629(3)	9 082(6)
Cl(1)	4 555(2)	4 012(1)	6 093(1)	C(123)	10 559(7)	3 577(3)	10 325(6)
Cl(2)	2 907(2)	3 373(1)	3 551(2)	C(124)	10 023(6)	3 677(3)	11 210(6)
Cl(3)	5 506(2)	2 700(1)	4 099(1)	C(125)	8 753(6)	3 833(3)	10 848(6)
P(1)	6 954(2)	3 334(1)	6 582(2)	C(126)	8 072(6)	3 882(2)	9 596(6)
P(2)	5 537(2)	3 904(1)	3 764(2)	C(131)	5 478(6)	2 667(2)	7 197(6)
O(11)	9 368(4)	3 480(2)	5 657(5)	C(132)	3 410(6)	2 545(3)	5 699(6)
O(13)	4 415(4)	2 879(2)	6 248(4)	C(133)	2 630(8)	2 425(4)	6 509(7)
O(21)	2 901(5)	4 964(2)	2 685(5)	C(211)	3 648(6)	4 617(3)	3 494(6)
O(23)	7 097(4)	4 676(2)	2 781(4)	C(212)	1 708(8)	4 813(5)	1 909(10)
C(11)	8 158(6)	2 929(2)	6 424(6)	C(213)	757(13)	4 907(5)	2 428(15)
C(12)	7 830(6)	3 856(2)	7 361(6)	C(221)	5 210(6)	3 580(2)	1 317(6)
C(13)	6 441(6)	3 047(3)	7 749(6)	C(222)	4 283(7)	3 232(3)	999(7)
C(21)	4 270(6)	4 283(2)	2 826(6)	C(223)	3 472(7)	3 190(3)	−220(6)
C(22)	6 133(6)	3 620(2)	2 627(5)	C(224)	3 582(8)	3 490(3)	−1128(7)
C(23)	6 816(6)	4 304(2)	4 584(6)	C(225)	4 496(8)	3 839(3)	−807(7)
C(111)	8 759(6)	3 034(2)	5 442(6)	C(226)	5 297(7)	3 892(3)	416(6)
C(112)	10 075(8)	3 567(3)	4 845(8)	C(231)	6 969(7)	4 761(3)	3 952(6)
C(113)	10 712(11)	4 027(4)	5 165(11)	C(232)	7 365(10)	5 111(3)	2 255(8)
C(121)	8 616(6)	3 782(2)	8 702(6)	C(233)	7 135(8)	5 055(3)	917(7)

in toluene (30 cm^3) was added a standard solution of L in light petroleum (2.2 cm^3, 2.16 mmol) and the yellow solution allowed to stir (12 h), during which time it changed to green. The solvents were removed *in vacuo* and the residue extracted into light petroleum (80 cm^3). After concentration of this solution to saturation (*ca.* 10–15 cm^3), air-stable pale yellow prisms of complex **4** were isolated in good yield (0.50 g, 66%). IR (Nujol mull): $\nu_{asym}(C_2O)$ 1105s; ν(CO) 1967s; ν(M–Cl) 305w cm^{-1}.

[Benzylbis(2-ethoxyethyl)phosphine]chloro(cyclooctadiene)-rhodium(I) **5**. To an orange solution of $[\{Rh(\mu\text{-}Cl)(cod)\}_2]$ (0.39 g, 1.58 mmol) in dichloromethane (50 cm^3) was added a standard solution of L in light petroleum (1.6 cm^3, 1.58 mmol), and the solution allowed to stir (6 h). After this time it had turned yellow, and the solvents were removed *in vacuo*. The oil/solid residue was extracted into hot light petroleum (200 cm^3), and after concentration to saturation, complex **5** was isolated as an air-stable pale orange solid in high yield (0.72 g, 89%). Mass spectrum (EI, CI): *m*/*z* 514 (M^+), 479 (*M* − Cl), 406 (*M* − cod), 370 (RhL), 268 (L), 122 ($PhCH_2P$), 108 (cod), 91 ($PhCH_2$) and 77 (Ph). IR (Nujol mull): $\nu_{asym}(C_2O)$ 1103s; ν(C=C, cod) 1600w (other peaks due to cod are either too weak or obscured by L peaks); ν(Rh–Cl) 280w cm^{-1}.

[Benzylbis(2-ethoxyethyl)phosphine]chloro(cyclooctadiene)-iridium(I) **6**. To an orange solution of $[\{Ir(\mu\text{-}Cl)(cod)\}_2]$ (0.14 g, 0.21 mmol) in toluene (20 cm^3) was added a standard solution of L in light petroleum (0.4 cm^3, 0.42 mmol), and the solution allowed to stir (12 h). After this time it had turned yellow, and the solvents were removed *in vacuo*. The oil/solid residue was extracted into light petroleum (100 cm^3), and after concentration to saturation, complex **6** was isolated as a reasonably air-stable orange solid in high yield (0.2 g, 80%). IR (Nujol mull): $\nu_{asym}(C_2O)$ 1103s; ν(C=C, cod) 1600w (other peaks due to cod are either weak or obscured by L peaks); ν(Ir–Cl) 300m cm^{-1}.

Reaction of Cyclohexene with Complex 3.—To a solution of complex **3** (0.1 g, 0.13 mmol) in $[^2H_8]$toluene (*ca.* 2 cm^3) in an NMR tube was added an excess of cyclohexene (0.1 cm^3, 1.3 mmol) and the variable-temperature $^{31}P\text{-}\{^1H\}$ NMR spectrum measured.

Single-crystal X-Ray Crystallography of Complexes 2 *and* 3.—Crystals of complex **2** were recrystallized from dichloromethane and of **3** from diethyl ether.

Crystal data. Complex **2**. $C_{32}H_{50}CoF_6O_{10}P_2S_2$, M_r = 893.71, monoclinic, *a* = 12.158(8), *b* = 10.960(7), *c* = 15.166(9) Å, β = 100.09(9)°, *U* = 1990(2) $Å^3$, space group $P2_1/c$ (no. 14), *Z* = 2, D_c = 1.492 g cm^{-3}, *F*(000) = 930, μ = 6.96 cm^{-1}, *T* = 120(2) K, pink prisms, crystal size *ca.* 0.144 × 0.07 × 0.07 mm.

Complex **3**. $C_{30}H_{50}Cl_3O_4P_2Rh$, M_r = 745.90, monoclinic, *a* = 11.1114(8), *b* = 28.386(8), *c* = 11.473(4) Å, β = 109.449(1)°, *U* = 3412(2) $Å^3$, space group $P2_1/n$ (alternative no. 14), *Z* = 4, D_c = 1.452 g cm^{-3}, *F*(000) = 1552, μ = 8.62 cm^{-1}, *T* = 140(2) K, orange needles, crystal size *ca.* 0.2 × 0.13 × 0.11 mm.

Data collection and processing.[30] Delft instruments FAST TV area detector diffractometer at the window of a rotating-anode FR591 generator (50 kV, 40 mA), with a molybdenum target [λ(Mo-Kα) = 0.710 69 Å], controlled by a MicroVax 3200 computer and driven by MADNES[31] software. The data sets were recorded at 120 (complex **2**) and 140 K (**3**) using an Oxford cryostream low-temperature cooling system. For **2**, 7424 reflections were collected (2.30 < θ < 25.07°), index ranges $-13 < h < 13$, $-10 < k < 13$, $-17 < l < 17$, giving 2980 unique data [R_{int} = 0.1393 after absorption correction (DIFABS)[32]]. For **3**, 8859 reflections were collected (2.01 < θ < 25.06°), index ranges $-13 < h < 12$, $-30 < k < 18$, $-12 < l < 13$, giving 4608 unique data [R_{int} = 0.0524 after absorption correction (DIFABS)[32]].

Structure analysis and refinement. Both structures were solved by heavy-atom methods (SHELXS[33]) and then subjected to full-matrix least-squares refinement based on F_o^2 (SHELX 93[34]). Non-hydrogen atoms were refined anisotropically, with all hydrogens included in idealized positions (C–H 0.97 Å, C/H–C–H 109.5°) with isotropic thermal parameters free to refine. Phenyl rings were idealized as regular hexagons (C–C 1.395 Å, C–C–C 120°). The weighting scheme used was $w = 1/[\sigma^2(F_o^2)]$. For complex **2**, final wR_2 and R_1 values* were 0.1409 and 0.1552 respectively, for all 2970 data and 243 parameters (ρ_{max}, ρ_{min} 0.499, −0.363 e $Å^{-3}$). The corresponding wR_2 and R_1 values [$I > 2\sigma(I)$] were 0.0970 and 0.0497 respectively. For **3**, final wR_2 and R_1 were 0.1333 and 0.0761 respectively, for all 4608 data and 426 parameters (ρ_{max}, ρ_{min} 0.421, −0.509 e $Å^3$). The corresponding wR_2 and R_1 values [$I > 2\sigma(I)$] were 0.0790 and 0.0309 respectively.

Diagrams were drawn with SNOOPI.[35] All calculations were performed on a 486DX2/66 personal computer. Sources of scattering factor data are given in ref. 34.

---

* $wR_2 = \{\Sigma[w(F_o^2 - F_c^2)^2]/\Sigma[w(F_o^2)^2]\}^{\frac{1}{2}}$, $R_1 = \Sigma(F_o - F_c)/\Sigma(F_o)$.

Additional material available from the Cambridge Crystallographic Data Centre comprises H-atom coordinates, thermal parameters, and remaining bond lengths and angles.

Acknowledgements

We thank the EPSRC and BP Chemicals Ltd. for a CASE studentship (to S. J. C.), and to EPSRC for support to the crystallography unit. Grateful thanks are due to Dr. W. O. Howarth for the acquisition of NMR spectra and the EPSRC for access to this facility. We also thank Dr. J. A. Ballantine and the EPSRC service for mass spectra.

References

1 For example, see (*a*) A. Bader and E. Lindner, *Coord. Chem. Rev.*, 1991, **108**, 27 and refs. therein; (*b*) E. Lindner, J. Dettinger and A. Möckel, *Z. Naturforsch., Teil B*, 1991, **46**, 1519; (*c*) E. Lindner and J.-P. Reber, *Z. Naturforsch., Teil B*, 1991, **46**, 1581; (*d*) E. Lindner, A. Möckel, H. A. Mayer and R. Fawzi, *Chem. Ber.*, 1992, **125**, 1363; (*e*) E. Lindner, A. Möckel, H. A. Mayer, H. Kühbauch, R. Fawzi and M. Steimann, *Inorg. Chem.*, 1993, **32**, 1266; (*f*) E. Lindner, Q. Wang, H. A. Mayer, A. Bader, H. Kühbauch and P. Wegner, *Organometallics*, 1993, **12**, 3291; (*g*) M. R. Mason, Y. Su, R. A. Jacobson and J. G. Verkade, *Organometallics*, 1991, **10**, 2335; (*h*) H. Werner, A. Hampp and B. Windmüller, *J. Organomet. Chem.*, 1992, **435**, 169; (*i*) M. A. Esteruelas, A. M. López, L. A. Oro, A. Perez, M. Schulz and H. Werner, *Organometallics*, 1993, **12**, 1823.

2 W. Keim, *Chem.-Ing.-Tech.*, 1984, **56**, 850.

3 E. Lindner, J.-P. Reber and P. Wegner, *Z. Naturforsch., Teil B*, 1988, **43**, 1268.

4 E. Lindner, A. Sickinger and P. Wegner, *J. Organomet. Chem.*, 1988, **349**, 75.

5 E. Lindner, U. Schrober, E. Glaser, H. Norz and P. Wegner, *Z. Naturforsch., Teil B*, 1987, **42**, 1527.

6 E. Lindner, H. A. Mayer and P. Wegner, *Chem. Ber.*, 1986, **119**, 2616.

7 S. J. Chadwell, S. J. Coles, P. G. Edwards, M. B. Hursthouse and A. Imran, *Polyhedron*, 1995, **14**, 1057.

8 N. N. Greenwood and A. Earnshaw, *Chemistry of the Elements*, 1st edn., Pergamon, Oxford, 1984, p. 1315.

9 F. A. Cotton, O. Faut, D. M. L. Goodgame and R. H. Holm, *J. Am. Chem. Soc.*, 1961, **83**, 1780.

10 S. P. Gejji, K. Hermansson and J. Lindgren, *J. Phys. Chem.*, 1993, **97**, 3712.

11 G. A. Lawrence, *Chem. Rev.*, 1986, **86**, 17.

12 S. D. Brown and G. L. Gard, *Inorg. Chem.*, 1975, **14**, 2273.

13 J. R. Dalziel and F. Aubke, *Inorg. Chem.*, 1973, **12**, 2707.

14 E. Lindner, Q. Wang, H. A. Mayer, R. Fawzi and M. Steimann, *Organometallics*, 1993, **12**, 1865.

15 D. F. Evans, *J. Chem. Soc.*, 1959, 2003.

16 R. C. Elder, *Inorg. Chem.*, 1968, **7**, 1117; J. Estienne and R. Weiss, *J. Chem. Soc., Chem. Commun.*, 1972, 862.

17 M.-T. Youinou, R. Ziessel and J.-M. Lehn, *Inorg. Chem.*, 1991, **30**, 2144.

18 P. L. Orioli, *Coord. Chem. Rev.*, 1971, **6**, 285; M. Ciampolini, P. Dapporto, N. Nardi and F. Zanobini, *J. Chem. Soc., Chem. Commun.*, 1980, 177; A. Bianchi Orlandio, C. Calabresi, C. A. Ghilardi, P. L. Orioli and L. Sacconi, *J. Chem. Soc., Dalton Trans.*, 1973, 1383.

19 A. R. H. Al-Soudani, A. S. Batsanov, P. G. Edwards and J. A. K. Howard, *J. Chem. Soc., Dalton Trans.*, 1994, 987.

20 V. G. Albano, P. L. Bellon and G. Ciani, *J. Organomet. Chem.*, 1972, **38**, 155.

21 (*a*) P. Braunstein, D. Matt, F. Mathey and D. Thavard, *J. Chem. Res. (S)*, 1978, 232; (*b*) J. G. Verkade, *Coord. Chem. Rev.*, 1972–1973, **9**, 1; (*c*) D. A. Knight, D. J. Cole-Hamilton, D. C. Cupertino, M. Harman and M. B. Hursthouse, *Polyhedron*, 1992, **11**, 1987.

22 P. Braunstein, D. Matt, F. Mathey and D. Thavard, *J. Chem. Res.*, 1978 (*S*) 232; (*M*) 3041.

23 P. Braunstein, Y. Chauvin, J. Nähring, A. DeCian and J. Fischer, *J. Chem. Soc., Dalton Trans.*, 1995, 863.

24 A. C. Skapski and F. A. Stephens, *J. Chem. Soc., Dalton Trans.*, 1973, 1789.

25 C. Brown, B. T. Heaton, L. Longhetti, W. T. Povey and D. O. Smith, *J. Organomet. Chem.*, 1980, **192**, 93.

26 R. P. Hughes, in *Comprehensive Organometallic Chemistry*, eds. G. Wilkinson, F. G. A. Stone and E. W. Abel, Pergamon, New York, 1982, vol. 5, ch. 35, pp. 296–307.

27 R. Cramer, *Inorg. Synth.*, 1974, **15**, 14.

28 G. Giordano and R. H. Crabtree, *Inorg. Synth.*, 1979, **19**, 218.

29 J. L. Herde, J. C. Lambert and C. V. Senoff, *Inorg. Synth.*, 1974, **15**, 18.

30 S. R. Drake, M. B. Hursthouse, K. M. A. Malik and S. A. S. Miller, *Inorg. Chem.*, 1993, **32**, 4653.

31 J. W. Pflugrath and A. Messerschmidt, MADNES, version 11, September 1989, Delft Instruments, Delft, 1989.

32 N. P. C. Walker and D. Stuart, *Acta Crystallogr., Sect. A*, 1983, **39**, 158; adapted for FAST geometry by A. Karaulov, University of Wales, Cardiff, 1991.

33 G. M. Sheldrick, *Acta Crystallogr., Sect. A*, 1990, **46**, 467.

34 G. M. Sheldrick, University of Göttingen, 1993, unpublished work.

35 K. Davies, University of Oxford, 1983, unpublished work.

Received 22nd *May* 1995; *Paper* 5/03263F